Synthesis of Biodegradable and Biocompatible Polymer Brushes with High Grafting Density on the Surface of Nano-hydroxyapatite by Combination of ATRP and ROP

Zeng Liang, Wang Haibo, Fu Guoxin, Jiang Jianwei, Zhang Xuefei
(College of Chemistry, Xiangtan University, Hunan Province, HuNan XiangTan 411105)

Abstract: A facile strategy for growing biodegradable and biocompatible polymer brushes with high grafting density on the surface of nano-hydroxyapatite (n-HAP) by combination of Atom Transfer Radical Polymerization (ATRP) and Ring-Opening Polymerization (ROP) will be presented. Firstly, ATRP was used to graft poly (2-hydroxyethyl methacrylate) (PHEMA) onto the n-HAP surface. Then, the hydroxyls groups introduced onto the n-HAP were used initiating the ROP of ε-caprolactone for constructing polymer brushes on the n-HAP. The functionalized n-HAP was characterized by FT-IR, 13C Solid-State Cross-Polarization Magic-Angle-Spinning (13C CP/MAS), Thermal Gravimetric Analysis (TGA), X-ray Diffraction (XRD), and Transmission Electron Microscopy (TEM) measurements. The measurement results demonstrated that the biodegradable and biocompatible polymer brushes have been grown successfully and the average thickness of grafted polymer layers can be controlled well by adjusting the feed ratio. This convenient strategy can be used extended to prepare other functional/multifunctional polymer brushes in the future and open an avenue for further grafting therapeutic molecules and other biomolecule on the n-HAP.

Keywords: Polymer Chemistry; Hydroxyapatite; Atom transfer radical polymerization; Ring-opening polymerization; Surface modification

0 Introduction

Nano-hydroxyapatite (n-HAP) has become one of the most important biomedical materials in replacement and drug carrier fields for its excellent biocompatibility, good bone bonding ability and no causing any systemic toxicity in human internal environment [1–7]. It can be bonded with bone protein directly and induce new bone growth for its highly similar with the major inorganic composition of natural bone[8]. Therefore, many researches have been made on its structure–property relationship and possible applications as biomaterials, such as bone filler [9], coating of orthopedic implants [10] and filler of inorganic/polymer composites [11]. To produce the composites with bonelike properties, the interaction and adhesion between the n-HAP filler and the polymer matrix are critical factor to determine the composites with good mechanical properties. This is because the lack of adhesion between inorganic fillers and the organic polymer matrix will result in an early failure at the interface and deteriorate the mechanical properties of composites [12–16]. Therefore, it is necessary to modify the surface properties of n-HAP by organic molecules or polymers to improve the compatibility between the filler and polymer matrix. Various methods have been developed to tune the surface properties of n-HAP, including the use of silane coupling agents [17], pyrophosphoric acid [18], dodecyl alcohol [19] and isocyanates [20]. In these methods, most of molecules were grafted on the surface of n-HAP through covalent bonds by the chemical reaction with the surface hydroxyl groups of n-HAP directly. However, the hydroxyl groups on the n-HAP surface with the limited reactivity are not effective enough to graft organic molecules with high grafting ratio [1,12]. For this reason, a facile strategy, which could be used to modify the surface of n-HAP with high grafting ratio, is an important subject. In this paper, we adopted to

Foundations: Specialized Research Fund for the Doctoral Program of Higher Education(20070530007)
Brief author introduction: Liang Zeng（1984-），man,student,functional polymer
Correspondance author: Xuefei Zhang（1975-），man,assosiate professor，biomedical material. E-mail: zxf7515@yahoo.com.cn

"grafting from" strategy and desire to construct biodegradable and biocompatible Polymer Brushes with high grafting density on the surface of n-HAP particles by combination of Atom Transfer Radical Polymerization (ATRP) and Ring-Opening Polymerization (ROP). The detailed procedure is shown in Scheme 1. In the first step, n-HAP was reacted with 2-bromoisobuturyl bromide (BIBB) directly, and then, the obtained product was used to initiate polymerization of the 2-hydroxyethyl methacrylate (HEMA) via ATRP. By this simple but effective way, the comb-shaped poly (ε-caprolactone) brushes on the surface of n-HAP particles with high grafting ratio would be constructed.

1 Materials and methods

1.1 Materials and reagents

Calcium hydroxide ($Ca(OH)_2$), phosphoric acid (H_3PO_4), 2, 2'-bipyridine (bpy), 2-hy droxyethyl methacrylate (HEMA), N,N-(dimethylamino)pyridine (DMAP, 98%), and stannous octoate ($Sn(Oct)_2$) were purchased from Aldrich and were used without further purification. 2-bromoisobuturyl bromide (BIBB) (98%, Alfa) was freshly distilled at room temperature under vacuum. ε-Caprolactone was dried over calcium hydride and distilled under reduced pressure before use. Tetrahydrofuran (THF) and toluene were distilled from Na/benzophenone under argon before use. Triethylamine (TEA) was refluxed with tosyl chloride to remove the primary amines and secondary amines, Cu(I)Br was washed by acetic acid and ethanol three times respectively and then dried under vacuum. All other reagents and chemicals were of the analytical grade.

1.2 Measurements

Fourier Transformation Infrared (FTIR) spectra were recorded on a Perkin-Elemer Spectrum one FTIR spectrophotometer, 32 scans were signal-averaged with a resolution of 2 cm^{-1} at room temperature. Samples were prepared by dispersing the complexes in KBr and compressing the mixtures to form disks. Thermal Gravimetric Analysis (TGA) was made using a 7 Series thermal analysis system (Perkin-Elmer). Samples were heated at 10 ℃/min from room temperature to 700℃ in a dynamic nitrogen atmosphere at a flow rate of 60 ml/min. 13C solid-state NMR were performed on a Bruker InfinityPlus 400 spectrometer operating at 100 MHz, by use of cross-polarization from a proton. The contact time was 0.400 m, the pulse delay 1 s, and the spinning rate 5 kHz. The wide angle X-ray diffraction (WAXD) data from 200 to 700 of the samples were measured using a Rigaku D/max 2500 kV PC X-Ray Diffractometer with a Cu tube anode. Transmission Electron Microscopy (TEM) was performed on a JEOL JEM-2010 (Tokyo, Japan), operating at an acceleration voltage of 200 kV. A drop of the sample solution in methylene chloride (concentration 0.5 g/L) was placed onto a 200-mesh copper grid coated with carbon. The samples were air-dried before measurement.

1.3 Synthesis of nano-hydroxyapatite (n-HAP) particles

The n-HAP particles were prepared by chemical precipitation according to the literature procedure [24]. A vigorously stirred aqueous solution of $Ca(OH)_2$ (0.25 mol/L, 1.35 L) was titrated with an aqueous of H_3PO_4 (0.30 mol/L, 0.60 L) dropwise at a rate of 1 mL/min at 60℃. After completion of H_3PO_4 addition, the pH of the suspension was adjusted to 7.0 with ammonium hydroxide.After aging for 24 h, the precipitation was purified by repeated washing with distilled water three times. The needlelike n-HAP particles of 100–150 nm in length and 20–30 nm in width were obtained by freeze-drying.

1.4 Coupling of the initiator to n-HAP particles (HAP–Br)

Firstly, 0.60 g dried n-HAP powder was added to a 50 mL flask containing 20 mL DMF solution, N,N-(dimethylamino) pyridine (DMAP) (0.06 g, 0.48 mmol), triethylamine (TEA) (0.61 g, 3.30 mmol) and it was ultrasonic vibrated for several minutes.Then 2-bromoisobuturyl bromide (BIBB) (0.60 g, 2.61 mmol) diluted in 10 mL of dried DMF was dropped into the flask gradually with ice bath. After completion of BIBB solution addition, the reaction was allowed to proceed with stirring for 24 h at room temperature.The product (HAP–Br) was washed with DMF and centrifugation at 2500 rpm for 20 min (5×). After that, the HAP–Br was washed with methylene chloride by Soxhlet extraction for 24 h. The HAP–Br was dried overnight under vacuum at 60℃, 0.63 g sample was obtained. The TGA result showed that the ATRP initiator had a functional group content of 0.31 mmol/g approximately.^{13}C CP/MAS (δ, ppm): 31.7 (-***C***H_3), 43.4 (-***C***$(CH_3)_2$-Br).

1.5 Synthesis of hydroxyl-group-functionalized n-HAP (HAP–PHEMA) via ATRP

Firstly, HAP-Br (1 g), Cu(I)Br (14.4 mg, 0.1 mmol), bpy (15.6 mg, 0.1 mmol), distilled water (0.5 mL), DMF (0.5 mL) and HEMA (1 g, 7.6 mmol) were introduced into a dry glass tube. And then the glass tube was degassed with three freeze-pump-thaw cycles and then sealed under vacuum. The tube was then placed in a thermo stated oil bath and left at 70 ℃ for 24 h. At the end of the reaction, the ungrafted free polymer, unreacted monomer, and catalyst were removed from the polymer-grafted nano-hydroxyapatite by washing repeated with solvent and centrifugation at 2500 rpm for 20 min (5×). The HAP-PHEMA (1: 1) (mass ratio of initiator/monomer) was dried overnight under vacuum at 60 ℃. Other HAP-PHEMA (1: 0.2) and HAP-PHEMA (1: 3) were obtained in an identical manner. ^{13}C MAS/NMR (δ): 67.6 $(-CH_2-O-)_{PHEMA}$, 60.5 $(-CH_2-OH)_{PHEMA}$, 55.4 $(-C(CH_3)Br-CO-)_{PHEMA}$, 51.4 $(-CH_2-)_{PHEMA}$, 30.1 $(-CH_3)_{PHEMA}$, 36.3 $(-CH_3)_{BIBB}$, 26.7 $(-CH_3)_{BIBB}$.

1.6 Removal of the activator contaminants

The copper contaminants were washed away from the greenish crude product by Soxhlet extraction with acetylacetone-ethanol solution (100 ml, volume ratio of 1: 3) for 48 h. The product was washed with ethanol and excess of water in turn. The white powder was obtained and it was dried overnight under vacuum at 60 ℃.

1.7 Constructing comb-shaped polymer brushes on the n-HAP via ROP

The dried HAP-PHEMA (1: 1) (0.1 g), ε-Caprolactone (0.1 g, 0.87 mmol) and $Sn(Oct)_2$ (0.045 g) were brought into a dried glass tube. The glass tube was degassed with three freeze-pump-thaw cycles and then sealed under vacuum. The tube was then placed in a thermo stated oil bath and left at 120 ℃ for several hours. At the end of the reaction the mixture was diluted with methylene chloride and the HAP-PHEMA(1:1)-$(PCL)_m$ was repeated washing-centrifugation cycle at 5000 rpm for 20 min (5×). The isolated was dried overnight under vacuum at 60 ℃. Other HAP-PHEMA(1:0.2)-$(PCL)_m$ and HAP-PHEMA(1:3)-$(PCL)_m$ were obtained in an identical manner. ^{13}C MAS/NMR (δ): 65.0-60.3 $(-O-CH_2CH_2-O-)_{PHEMA}$ and $(-CH_2-OH)_{PCL}$, 55.3 $(-CH_2-)_{PHEMA}$ and $(-C(CH_3)Br-CO-)_{PHEMA}$, 45.5 $(-C(CH_3)_2-)_{BIBB}$ and $(-C(CH_3)Br-CO-)_{PHEMA}$, 34.7 $(-CH_3)_{BIBB}$ and $(-CH_2-CO-)_{PCL}$, 28.4 $(-CH_2-CH_2OH)_{PCL}$, 25.5 $(-CH_3)_{PHEMA}$, 18.2-16.5 $(-CH_2CH_2-)_{PCL}$.

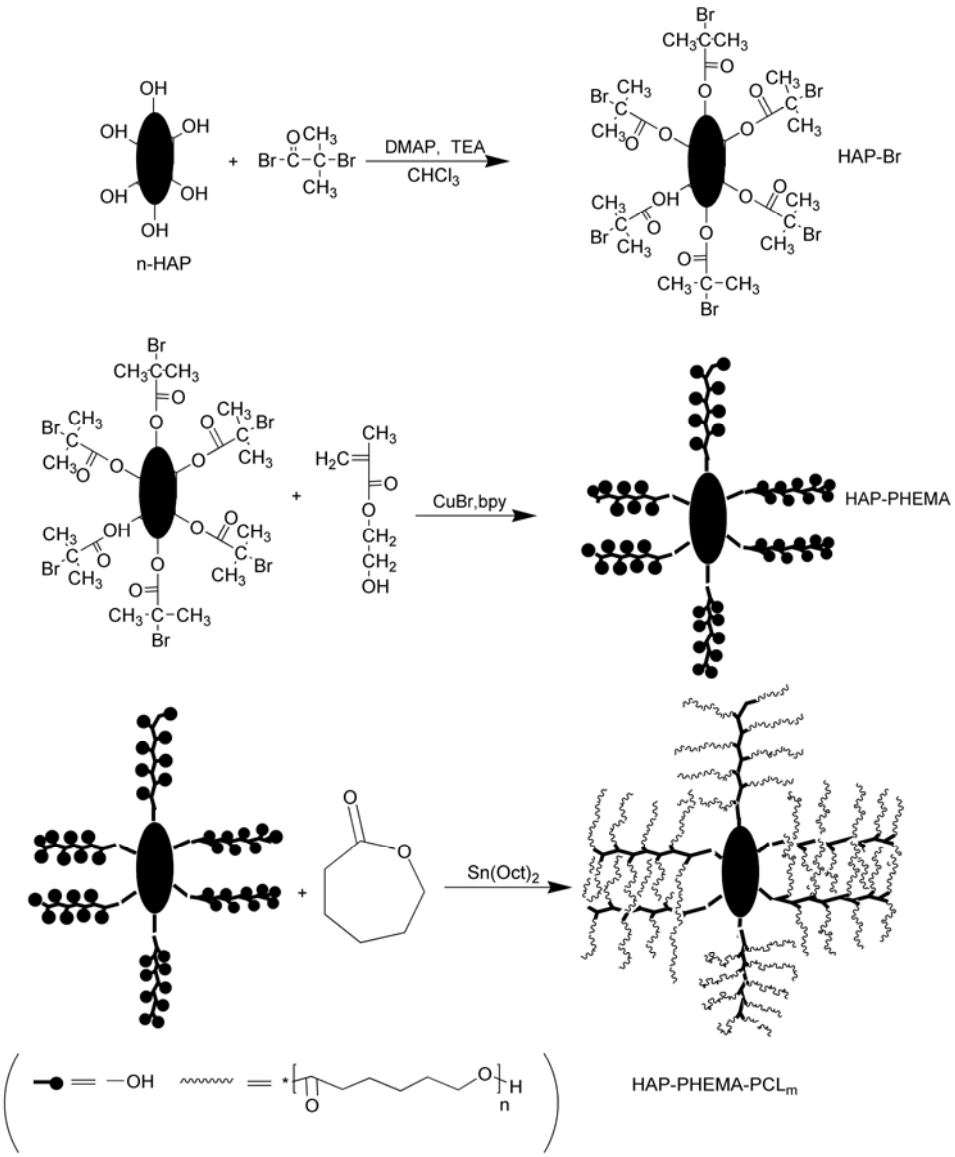

Scheme 1. Preparation of comb-shaped poly (ε-caprolactone) brushes from n-HAP.

2 Results and discussion

2.1 Preparation of ATRP initiator

To get ATRP initiators, the BIBB was employed to react with the surface hydroxyl groups of the n-HAP directly to prepare initiators. The FT-IR spectra of n-HAP and HAP–Br showed in Fig. 1. Compared with the spectrum of n-HAP, the new absorptions peak at 1575 cm^{-1} is observed in the spectrum of HAP–Br. This peak was attributed to the carbonyl groups vibration, implying the formation of covalent bond between n-HAP and BIBB. Solid-state ^{13}C NMR spectroscopy is a useful tool for characterizing the structures of the alkyl attached to the phosphate [27–29]. Two different carbons of BIBB are found in solid-state ^{13}C NMR spectrum of HAP–Br (Fig. 2). The obvious peak at 31.7 and 43.4 ppm were attributed to two different kinds of carbon of BIBB. In this figure, the quaternary carbon peak was located approximately 20 ppm downfield compared to that observed in solution [27], which further indicating the chemical reaction between n-HAP and BIBB had happened.

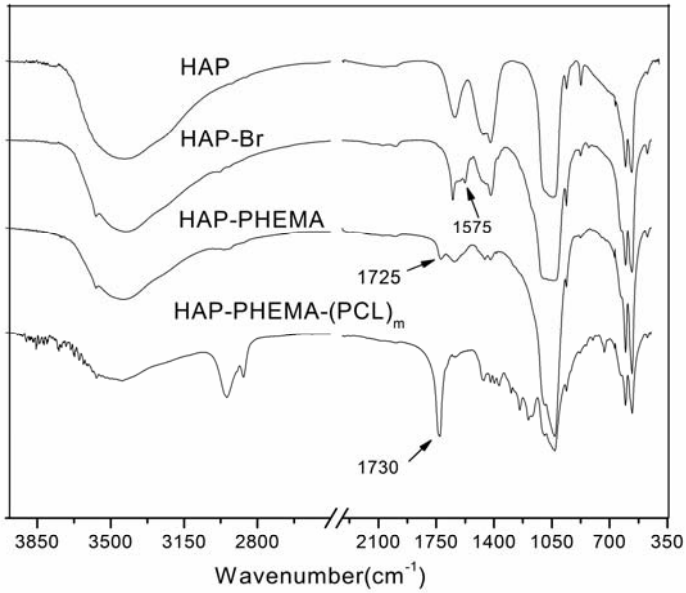

Fig. 1. FT-IR spectra of n-HAP, HAP–Br, HAP–PHEMA and HAP–HEMA–$(PCL)_m$, respectively.

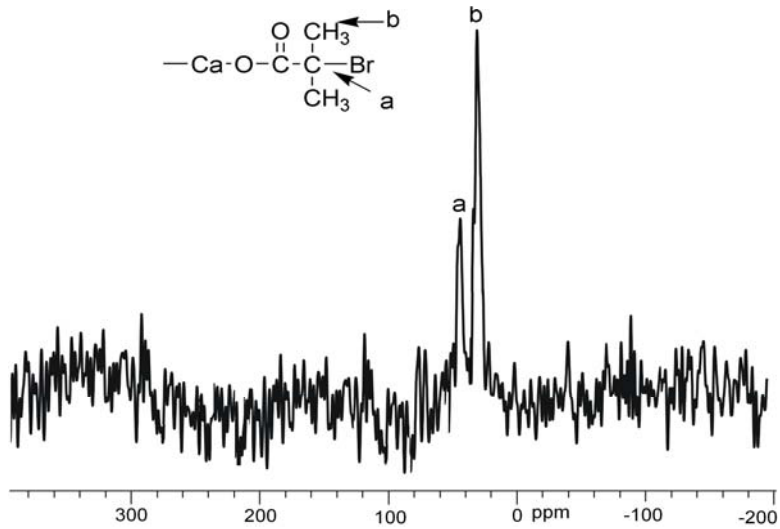

Fig. 2. ^{13}C magic-angle-spinning nuclear magnetic resonance spectrum of initiator grafted onto n-HAP (sample HAP–Br).

2.2 Growing comb-shaped polymer brushes on n-HAP surface

As described in the experimental section and Scheme 1, we firstly intended to graft polymer with hydroxyl groups via ATRP, then, the hydroxyl groups introduced onto the n-HAP were used to initiate the ROP of ε-caprolactone for constructing comb-shaped polymer brushes on the surface of n-HAP. The surface modified n-HAP was characterized by FT-IR, ^{13}C CP/MAS, TGA, XRD, and TEM measurements, respectively. In the FT-IR spectrum of HAP–PHEMA (Fig. 1), the characteristic peaks of carbonyl groups are observed at 1725 cm^{-1}, indicating the presence of ester bonds. In the ^{13}C CP/MAS trace for HAP–PHEMA (Fig. 3), the characteristic peaks belonging to

the carbons from PHEMA could be found. These results implied that the polymerization of HEMA had happened on the surface of n-HAP. After the ROP of ε-caprolactone, the new stronger absorption peaks at 1730 cm^{-1} and 2950 cm^{-1} in the FT-IR spectra of HAP–PHEMA–$(PCL)_m$ (Fig. 1) were clearly observed, respectively, which were assigned to the carbonyl and the alkyl groups of the PCL. Compared with Fig. 3, the ^{13}CCP/MAS spectra of the HAP–PHEMA–$(PCL)_m$ (Fig. 4) exhibited some characteristic peaks belonging to the carbons from PCL, in spite of the signals of the methylene groups from PHEMA and PCL overlapping together approximately at 30 ppm. Furthermore, evidence of grafting also can be seen by the downfield shift of the methylene carbon of PHEMA which appear at 51.4 ppm (C_g) in the ^{13}C MAS/NMR spectra of the HAP–PHEMA (Fig. 3) and is shifted to 65.0–60.3 ppm (C_f + C_g) in the ^{13}C MAS/NMR spectra of the HAP–PHEMA–(PCL)m (Fig. 4). As expected, the ROP propagates from the hydroxyl groups of the HEMA units along the copolymer backbone. All results confirm that the comb-shaped poly (ε-caprolactone) brushes had been grafted to the n-HAP surface successfully.

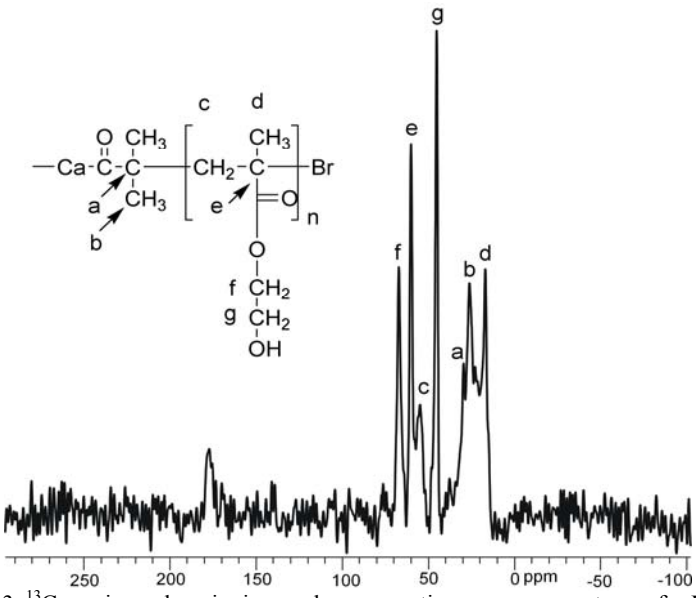

Fig. 3. ^{13}C magic-angle-spinning nuclear magnetic resonance spectrum of n-HAP after ATRP (sample HAP–PHEMA).

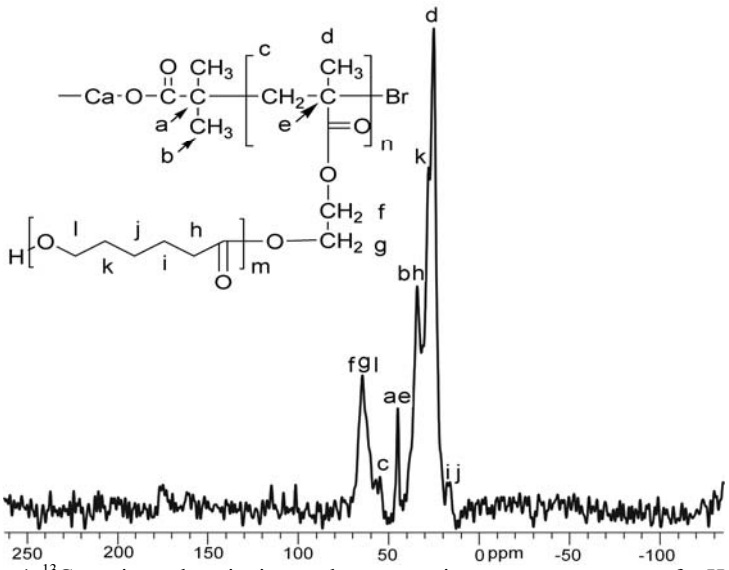

Fig. 4. ^{13}C magic-angle-spinning nuclear magnetic resonance spectrum of n-HAP after ATRP and ROP (sample HAP–PHEMA–$(PCL)_m$).

2.3 Thermal gravimetric analysis

The weight-loss of unmodified and modified n-HAP samples were investigated by employing TGA analysis in inert argon atmosphere. Fig. 5 and Fig. 6 displays the corresponding TGA weight-loss curves respectively. The weight losses of pure hydroxyapatite below 700 ℃ is less than 4.3%. It belongs to the adsorbed water in hydroxyapatite surface. Estimated from the TGA curves (Fig. 5), the amounts of grafted PHEMA was observed. The weight losses of ATRP initiator (HAP-Br) is about 6.68%. After grafting PHEMA on hydroxyapatite, the weight losses increased to 8.6%, 11.7% and 22.8%, respectively. These results demonstrated that the grafted functional polymer content can be well controlled via ATRP.

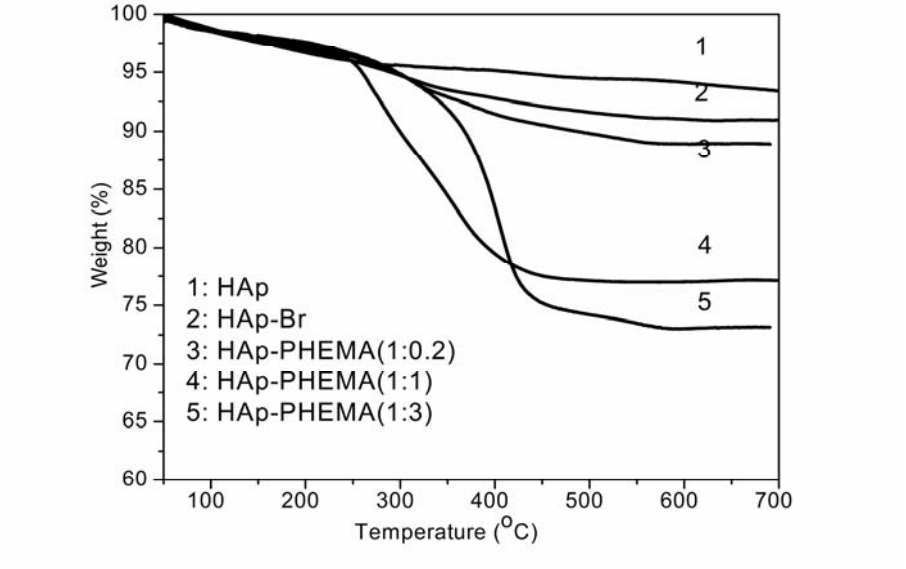

Fig. 5. TGA curves of n-HAP, HAP–Br, HAP–PHEMA (1:0.2), HAP–PHEMA (1:1), and HAP–PHEMA (1:3).

Fig. 6 displays the TGA curves of weight losses of the modified n-HAP after the ROP of ε-caprolactone on the surface of HAP–PHEMA particles. After growing comb-shaped polymer brushes, the weight losses increase to 19.52%, 45.30% and 55.87%, respectively. The results of grafting efficiency were summarized in Table 1: the maximum grafting efficiency of PCL is 63.70%, which means that the comb-shaped poly (ε-caprolactone) brushes have been grafted to the n-HAP surface with high grafting ratio successfully.

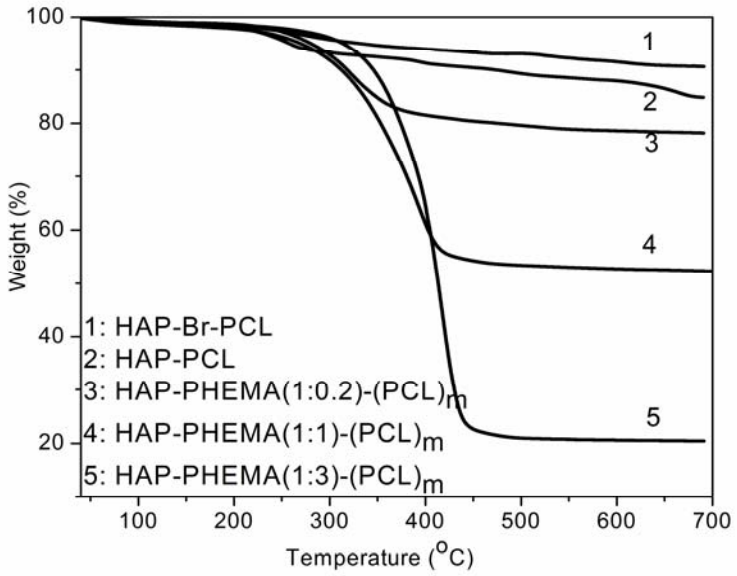

Fig. 6. TGA curves of HAP–PHEMA (1:0.2)–$(PCL)_m$, HAP–PHEMA (1:1)–$(PCL)_m$, and HAP–PHEMA (1:3)–$(PCL)_m$.

Table 1 TGA results of n-HAP, HAP–PHEMA, HAP–PHEMA–$(PCL)_m$, and their related parameters.

Materials	Feed ratio[a] HAP-Br/HEMA	Weight loss (M%)[b]	Graft amount (a%)[c]	Graft efficiency (*E*%)[d]
HAP	—	4.33	—	—
HAP-Br	—	6.95	2.62	—
HAP-PHEMA	1:0.2	8.84	1.89	10.37
HAP-PHEMA	1 : 1	11.68	4.73	5.36
HAP-PHEMA	1 : 3	24.30	17.35	7.64
HAP-PHEMA-$(PCL)_m$	1: 0.2	19.52	10.34	12.95
HAP-PHEMA-$(PCL)_m$	1 : 1	45.30	23.66	43.14
HAP-PHEMA-$(PCL)_m$	1 : 3	55.87	26.32	63.70
HAP-PCL	—	14.80	10.17	11.9
HAP-Br-PCL	—	9.69	7.07	7.8

[a] Feed ratio = HAP–Br:HEMA (wt:wt).
[b] Weight loss (M%) = weight fraction of grafted polymer calculated from TGA result.
[c] Graft amount (a%) = [HAP–PHEMA (M%)]–[HAP–Br (M%)] or [HAP–PHEMA–$(PCL)_m$ (M%)]–[HAP–PHEMA (M%)].
[d] Graft efficiency (E%) = graft amount/monomers used in polymerization.

2.4 Phase analysis by XRD

Powder X-ray diffraction (XRD) was used to characterize the crystallinity of unmodified and modified n-HAP samples. To keep its intrinsic properties, the surface modification of n-HAP should occur only at the n-HAP surface. In other words, the n-HAP should not change after it is treated by the surface modification method. It is necessary to demonstrate whether the maintenance of crystalline properties of HAP. The XRD patterns of n-HAP, HAP-Br, HAP-PHEMA and HAP-PHEMA-$(PCL)_m$ are shown in Fig. 7. By comparing with the standard cards (JCPDS no. 09-432 for HAP), the characteristic diffractions of (002), (102), (211), (300), (202), (310), (222), (213), and (411) indicated the crystalline phase of n-HAP nanocrystals. And as show in this figure, the ATRP and ROP did not induce change in crystalline phase of nanocrystals. This result supports that the polymerization only took place at the surface of nanocrystals without changing the bulk properties of n-HAP.

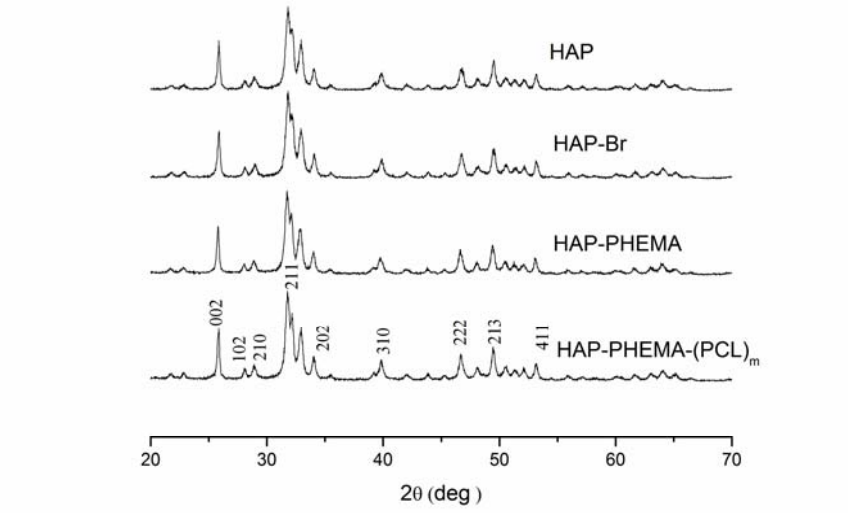

Fig. 7. XRD patterns of: (a) n-HAP, (b) HAP–Br, (c) HAP–PHEMA and (d) HAP–PHEMA–$(PCL)_m$.

2.5 TEM observation

Fig. 8 shows the TEM micrographs of unmodified n-HAP and the polymer-grafted n-HAP (n-HAP, HAP–PHEMA, HAP–PHEMA–$(PCL)_m$) of which TEM samples were prepared from the solutions of methylene chloride. It was found that the unmodified n-HAP had a strong tendency to aggregate and stacked together, individual n-HAP particles could hardly be found (Fig. 8A). However, after PHEMA was grafted to the surface of n-HAP via ATRP, the grafted n-HAP showed a nanorod shape and a much improved dispersion property (Fig. 8B). Besides, the modified n-HAP had a look of nanorod and exhibited the most excellent dispersion property in methylene chloride when the n-HAP particles were grafted with PHEMA and PCL via ATRP and ROP, furthermore, every particle was independent (Fig. 8C).

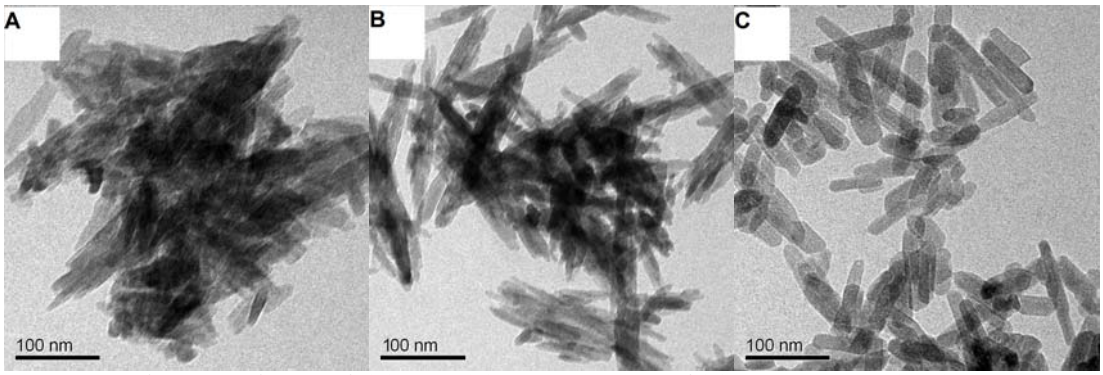

Fig. 8. TEM images of: (A) HAP, (B) HAP–PHEMA, and (C) HAP–PHEMA–$(PCL)_m$.

2.6 Dispersion test

In order to estimate the surface properties of the modified n-HAP, monitoring of time-dependent colloidal stability of HAP, HAP–PHEMA and HAP–PHEMA–$(PCL)_m$ in DMF and methylene chloride were illustrated in Fig. 9. The n-HAP nanoparticles precipitated in methylene chloride and DMF immediately, but the n-HAP modified with PHEMA and PHEMA–$(PCL)_m$

exhibited excellent colloid stability and could maintain a stable dispersion in suspension for 1 week in DMF. It is interesting to note that the n-HAP modified with PHEMA could not maintain stability and deposit in methylene chloride quickly. However, the n-HAP grafted with PHEMA–$(PCL)_m$ could be dispersed and remain stable very well in methylene chloride. This is because that there were many hydroxyl groups at the side chain of the grafted PHEMA, causing the surface properties of the n-HAP were hydrophilic, and the n-HAP nanoparticles changed from being hydrophilic to being hydrophobic when the HAP–PHEMA was grafted with PCL via ROP. The results means that we can easily obtained the modified n-HAP with the different surface properties by controlling the kind of the grafted polymer, which may be useful in the future to prepare the n-HAP/polymer composites when using different polymer matrix.

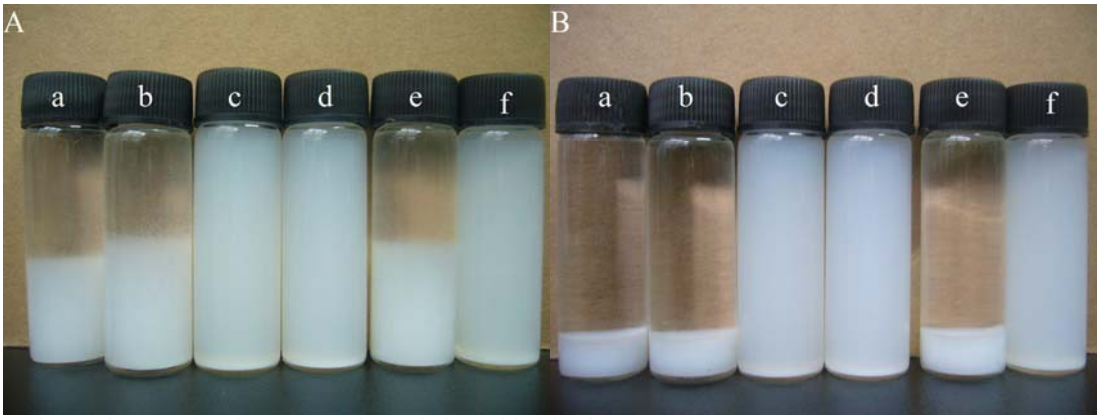

Fig. 9. Photographs of: (a) n-HAP in methylene chloride, (b) n-HAP in DMF, (c) HAP–PHEMA in DMF, (d) HAP–PHEMA–$(PCL)_m$ in DMF, (e) HAP–PHEMA in methylene chloride,(f) HAP–PHEMA in methylene chloride: (A) 10 min, (B) 24 h.

3 Conclusions

In this study, a versatile grafting strategy combining ATRP and ROP for modifying nano-hydroxyapatite surface has been presented. The chemical linkages were formed between hydroxyl on the surface of n-HAP and the carboxyl groups of 2-bromoisobuturyl bromide. The grafting strategy shows various advantages: (1) the functional group can be grafted on the HAP surface and became one part of it after immobilizing on n-HAP, (2) it is effective and convenient to construct different polymer brushes on hydroxyapatite surface, (3) different types of polymer brushes can grow on n-HAP via adopting different monomer, (4) the grafted weight ratios could be controlled discretionarily by adjusting the feed ratio of initiator and monomer. Therefore, both ATRP and ROP techniques can be combined to design polymer brushes according to specific requirements, opening a new strategy to functionalize n-HAP. This versatile modification of the n-HAP has shown great potential for future application in the tissue engineering and other medical applications. The extension of substrates and polymerization is in progress and will be reported.

4 Acknowledgements.

The authors are grateful to National Natural Science Foundation of China (20804032), Specialized Research Fund for the Doctoral Program of Higher Education(20070530007), Natural Science Foundation of Hunan Province of China (No. 06JJ20092) and Scientific Research Fund of Hunan Provincial Education Department(09K038).

References

[1] H.J. Lee, H.W. Choi, K.J. Kim, S.C. Lee. Modification of Hydroxyapatite Nanosurfaces for Enhanced Colloidal Stability and Improved Interfacial Adhesion in Nanocomposites[J]. Chem. Mater, 2006, 18(21): 5111-5118.
[2] M.C. Durrieu, S. Pallu, F. Guillemot, R. Bareille, J. Amédée, C.H. Baquey, C. Labrugère, M. Dard.Grafting RGD containing peptides onto hydroxyapatite to promote osteoblastic cells adhesion[J]. J. Mater. Sci.: Mater. Med, 2004,15(7):779-786.
[3] Jie, S.; Viengkham, M.; Carolyn, R. B. Mineralization of Synthetic Polymer Scaffolds: A Bottom-Up Approach for the Development of Artificial Bone[J]. J Am Chem Soc, 2005, 127 (10): 3366-3372.
[4] W. Guobao, P.X. Ma. Structure and properties of nano-hydroxyapatite/polymer composite scaffolds for bone tissue engineering[J]. Biomaterials, 2004, 25 (19): 4749-4757.
[5] L.L. Hench, J. Wilson.Surface-active biomaterials[J]. Science, 1984, 226: 630-636.
[6] T. Kitsugi, T. Yamamuro, T. Nakamura, S. Kotani, T. Kokubo, H. Takeuchi. Four calcium phosphate ceramics as bone substitutes for non-weight-bearing[J]. Biomaterials, 1993, 14(3): 216-224.
[7] J.D. Hartgerink, E. Beniash, S.I. Stupp. Self-Assembly and Mineralization of Peptide-Amphiphile Nanofibers[J]. Science, 2001, 294:1684-1688.
[8] R. Murugan; S. Ramakrishna. Bioresorbable composite bone paste using polysaccharide based nano hydroxyapatite[J].Biomaterials, 2004, 25(17): 3829-3835.
[9] J. Wilson, S.B. Low. Bioactive ceramics for periodontal treatment: Comparative studies in Patus monkeys[J]. J. Appl. Biomater., 1992, 3 (2): 123-129.
[10] K. Groot, R. Geesink, C.P.A.T. Klein, P. Serekian Plasma sprayed coatings of hydroxylapatite[J]. J. Biomed. Mater. Res., 1987, 21 (12): 1375-1381.
[11] R. Labella, M. Braden, S. Deb. Novel hydroxyapatite-based dental composites[J]. Biomaterials, 1994, 15 (15):1197-1200.
[12] X.Y. Qiu, Z.K. Hong, J.R. Sun, M.X. Deng, X.S. Chen, X.B. Jing. Hydroxyapatite Surface Modified by L-Lactic Acid and Its Subsequent Grafting Polymerization of L-Lactide[J]. Biomacromolecules, 2005, 6(3): 1193-1199.
[13] S.H. Pak, C. Caze. Acid-base interactions on interfacial adhesion and mechanical responses for glass-fiber-reinforced low-density polyethylene[J]. J. Appl. Polym. Sci., 1997, 65 (1): 143-154.
[14] W. Qiu, M. Kancheng, H. Zeng. Effect of macromolecular coupling agent on the property of PP/GF composites[J]. J. Appl. Polym. Sci., 1999, 71 (10):1537-1542.
[15] J.I. Velasco, J.A. De Saja, A.B. Martinez. Crystallization behavior of polypropylene filled with surface-modified talc[J]. J. Appl. Polym. Sci., 1996, 61 (1): 125-132.
[16] Z. Demjen, B. Pukanszky. J. Nagy. Possible coupling reactions of functional silanes and polypropylene[J]. Polymer, 1999, 40 (7): 1763-1773.
[17] J.C. Wei, A.X. Liu, L. Chen, P.B. Zhang, X.S. Chen, X.B. Jing. The Surface Modification of Hydroxyapatite Nanoparticles by the Ring Opening Polymerization of γ-Benzyl-L-glutamate N-carboxyanhydride[J]. Macromol. Biosci. 2009, 9 (7): 631-638.
[18] H. Tanaka, M. Futaoka, R. Hino. Surface modification of calcium hydroxyapatite with pyrophosphoric acid[J]. J. Colloid Interface Sci., 2004, 269 (2): 358-363.
[19] L. Borum-Nicholas, O.C. Wilson Jr.. Surface modification of hydroxyapatite. Part I. Dodecyl alcohol[J]. Biomaterials, 2003, 24 (21): 3671-3679.
[20] Q. Liu, C.A. van Blitterswijk. A study on the grafting reaction of isocyanates with hydroxyapatite particles[J]. J. Biomed. Mater. Res., 1998, 40 (3): 358-364.
[21] K. Matyjaszewski, J.H. Xia. Atom Transfer Radical Polymerization[J]. Chem. Rev., 2001,101 (9): 2921-2990.
[22]H. Kong, C. Gao, D.Y. Yan. Constructing amphiphilic polymer brushes on the convex surfaces of multi-walled carbon nanotubes by in situ atom transfer radical polymerization[J]. J. Mater. Chem, 2004, 14:1401-1405.
[23] H. Kong, C. Gao, D.Y. Yan. Controlled Functionalization of Multiwalled Carbon Nanotubes by in Situ Atom Transfer Radical Polymerization[J]. J. Am. Chem. Soc, 2004, 126 (2): 412-413.
[24]Y.B. Li, J. de Wijn, C.P.A.T. Klein, S. Van de Meer. Preparation and characterization of nanograde osteoapatite-like rod crystals[J].J. Mater. Sci.: Mater. Med, 1994, 5: 252-255.
[25] P. Liu, T.M. Wang. Poly (hydroethyl acrylate) grafted from ZnO nanoparticles via surface-initiated atom transfer radical polymerization[J]. Curr. Appl. Phys, 2008, 8 (1): 66-70.
[26] P. Liu, Y.H. Liu, Z.X. Su. Modification of Poly (hydroethyl acrylate)-Grafted Cross-linked Poly(vinyl chloride) Particles via Surface-Initiated Atom-Transfer Radical Polymerization (SI-ATRP). Competitive Adsorption of Some Heavy Metal Ions on Modified Polymers[J]. Ind. Eng. Chem. Res, 2006, 45 (7): 2255-2260.
[27] S. Haque, I. Rehman, J.A. Darr. Synthesis and Characterization of Grafted Nanohydroxyapatites Using Functionalized Surface Agents[J]. Langmuir, 2007, 23 (12):6671-6676.
[28] O.G. Silva, E.C. da Silva Filho, M.G. Fonseca, L.N.H. Arakaki, C. Airoldi. Hydroxyapatite organofunctionalized with silylating agents to heavy cation removal[J]. J. Colloid Interface Sci., 2006,302 (2): 485-491.
[29] A.A. Campbell, G.E. Fryxell, J.C. Linehan, G.L. Graff. Surface-induced mineralization: A new method for producing calcium phosphate coatings[J]. J. Biomed. Mater. Res., 1996, 32 (1): 111-118.
[30] H.W. Choi, H.J. Lee, K.J. Kim, H.M. Kim, S.C. Lee. Surface modification of hydroxyapatite nanocrystals by grafting polymers containing phosphonic acid groups[J]. J. Colloid Interface Sci., 2006, 304 (1): 277-281.

纳米羟基磷灰石表面构筑分子刷的新方法

曾亮，王海波，付国鑫，姜建伟，张雪飞
（湘潭大学化学学院，湖南 湘潭 411105）

摘要：一种通过结合原子转移自由基聚合(ATRP)和开环聚合(ROP)在纳米羟基磷灰石表面结合接枝高密度聚合物分子刷的常规方法。首先，通过 ATRP 成功将聚甲基丙烯酸甲酯接枝在纳米羟基磷灰石表面。然后通过引入的表面羟基引发己内酯的开环聚合从而构建具有聚合物分子刷的纳米羟基磷灰石。功能团化的纳米羟基磷灰石采用 13C 固体核磁(13C CP/MAS),热失重分析(TGA)，X 射线衍射(XRD)及透射电镜(TEM)进行了表征。这些手段表明生物可降解和生物相容性的聚合物分子刷成功接枝上并且可以通过投料比来有效控制和调整接枝率。这种简单方法可以用来对纳米粒子单/多功能化，为进一步在纳米羟基磷灰石表面接枝药物分子及其它生物分子提供了一种全新途径。

关键词：高分子化学；羟基磷灰石；原子转移自由基聚合；开环聚合；表面改性

中图分类号：CSO-O63